Biochimica et Biophysica Acta 1840 (2014) 3335–3344

Contents lists available at ScienceDirect

Biochimica et Biophysica Acta

journal homepage: www.elsevier.com/locate/bbagen

SH2B1 increases the numbers of IRSp53-induced filopodia

Shao-Jing Hong [a,1], Szu-Ting Liu [a,1], Chien-Jen Chen [a], Linyi Chen [a,b,*]

[a] Institute of Molecular Medicine, National Tsing Hua University, Hsinchu 30013, Taiwan, ROC
[b] Department of Medical Science, National Tsing Hua University, Hsinchu 30013, Taiwan, ROC

ARTICLE INFO

Article history:
Received 23 April 2014
Received in revised form 19 August 2014
Accepted 21 August 2014
Available online 28 August 2014

Keywords:
Filopodia
Membrane protrusion
IRSp53
SH2B1

ABSTRACT

Background: Filopodia are actin-rich membrane protrusions that play instrumental roles in development, cell migration, pathogen detection, and wound healing. During neurogenesis, filopodium formation precedes the formation of dendrites and spines. The insulin receptor substrate protein of 53 kDa (IRSp53) has been implicated in regulating the formation of filopodia. Our previous results suggest that a signaling adaptor protein SH2B1β is required for neurite outgrowth of hippocampal neurons and neurite initiation of PC12 cells. Thus, we hypothesize that IRSp53 and SH2B1β may act together to regulate filopodium formation.
Methods: To determine the contribution of IRSp53 and SH2B1β in the formation of filopodia, we transiently transfect IRSp53 and/or SH2B1β to 293T cells. Cell morphology and protein distribution are assessed via confocal microscopy and subcellular fractionation. Total numbers of filopodia and filopodium numbers per perimeter are calculated to show the relative contribution of IRSp53 and SH2B1β.
Results: In this study, we show that SH2B1β interacts with IRSp53 and increases the number of IRSp53-induced filopodia. One mechanism for this enhancement is that IRSp53 recruits SH2B1β to the plasma membrane to actively promote membrane protrusion. The increased numbers of filopodia likely result from SH2B1-mediated cytoplasmic extension and thus increased cell perimeter as well as IRSp53-mediated filopodium formation.
Conclusions: Taken together, this study provides a novel finding that SH2B1β interacts with IRSp53-containing complexes to increase the number of filopodia.
General significance: A better understanding of how SH2B1β and IRSp53 promote filopodium formation may have clinical implication in neurogenesis and regeneration.

1. Introduction

The actin cytoskeleton maintains cellular shape and plays an important role in many cellular processes such as adhesion, migration, endocytosis, phagocytosis and neurite outgrowth [1–3]. Filopodia are actin filaments arranged to form finger-like membrane protrusions [4]. Filopodia function by sensing environmental cues, serving as sites for integrating signaling and interacting with extracellular matrix (ECM). Small GTPase members of the Rho superfamily are known to regulate the dynamics of actin cytoskeleton [5]. Activated Cdc42 activates Arp2/3 actin nucleation complex to promote actin polymerization, via interaction with WASP (Wiskott Aldrich Syndrome protein) and N-WASP (Neuronal-WASP) [6].

IRSp53, a downstream effector of Cdc42, was originally identified in a screen for phosphorylation targets of the insulin receptor [7], but the subsequent studies focused on its role in the formation of filopodia [8–12]. IRSp53 belongs to the IMD [IRSp53 and missing in metastasis (MIM) homology domain] domain-containing protein family which share a well conserved N terminal helical IMD [13], which interact with phospholipids and generate membrane deformation [14,15]. IMD domain is also known as the I-BAR (inverse BAR) domain. The IMD/I-BAR domain of IRSp53 generates negative membrane curvature to induce plasma membrane protrusions [16]. IRSp53 also contains a half-CRIB motif known to bind to active form Cdc42 but not Rac [9]. The SH3 domain of IRSp53 has been shown to bind to various proline rich-containing proteins, including WAVE2 (Wiskott–Aldrich syndrome protein family verprolin homologue 2), Mena/VASP (Mammalian enabled/Vasodilator-stimulated phosphoprotein), espin, Eps8 (epidermal growth factor receptor pathway substrate 8), ProSAP/Shank, DRLPA (Dentatorubral-pallidoluysian atrophy) and synaptopodin [9,12,17–24]. Full-length IRSp53 is auto-inhibited and can be activated synergistically through binding of Cdc42 to CRIB domain and effector proteins to the SH3 domain [25]. Thus, the IMD and the SH3 domains are essential for IRSp53-mediated actin assembly. Nonetheless, how SH3 interactors target to membrane and regulate actin filaments remain unclear.

As IRSp53 has been implicated in binding with many actin modifiers. A central question is how IRSp53 regulates cytoskeleton remodeling and thus cell morphology. Evidence suggests that interaction between

* Corresponding author at: Institute of Molecular Medicine and Department of Medical Science, National Tsing Hua University, 101, Section 2, Kuang-Fu Road, Hsinchu 30013, Taiwan, ROC. Tel.: +886 3 5742775; fax: +886 3 5715934.
E-mail address: lchen@life.nthu.edu.tw (L. Chen).
[1] These two authors contribute equally.

http://dx.doi.org/10.1016/j.bbagen.2014.08.011
0304-4165/

IRSp53 and the actin capping protein Eps8 promotes actin filament bundling and thus the formation of filopodia [12]. Cdc42 also plays a role in enhancing the crosslinking activity of IRSp53–Eps8 complex during the formation of filopodia [12]. This result suggests that actin filament bundling is essential to produce filopodia.

SH2B1 belongs to SH2B family members, including SH2B1 (SH2-B, PSM), SH2B2 (APS), and SH2B3 (Lnk), is an adaptor protein that regulates several signaling pathways [26–35]. These family members contain amino (N)-terminal dimerization domain, proline-rich domains, pleckstrin homology (PH) domain and a carboxyl (C)-terminal Src homology 2 (SH2) domain. Four SH2B1 splice variants, α, β, γ and δ, have been identified so far [26,27,36]. SH2B1 promotes neurite initiation, outgrowth and neuronal survival of PC12 cells, cortical and hippocampal neurons [31,35,37,38]. Besides general function as a signaling adaptor protein, SH2B1β also acts as a nuclear protein which shuttles between cytosol and nucleus to regulate expression of genes such as MMP3, MMP10, uPAR, Egr1 and Cdh2 [39–41]. In addition to promote cell differentiation and survival, SH2B1 is involved in actin-based motility [42]. SH2B1 also acts as a cross-linker to regulate actin cytoskeleton organization [43]. Based on the known function of SH2B1 in neurite formation and the fact that filopodium formation precedes neurite initiation [44], we test the hypothesis that SH2B1 promotes the formation of filopodia.

2. Materials and methods

2.1. Reagents

Polyclonal antibody to rat SH2B1 was raised against a glutathione S-transferase fusion protein containing amino acids 527–670 of SH2B1β as described previously [28] and was a gift from Professor Christin Carter-Su from the University of Michigan, USA and used at a dilution of 1:1000 for western blotting. Dulbecco's modified Eagle's medium (DMEM), fetal bovine serum (FBS), horse serum (HS), L-glutamine (L-Gln), antibiotic-antiMycotic (AA), Alexa-Flour 555-conjugated goat anti-mouse antibody, Alex-Flour 488-conjugated goat anti-rabbit antibody, Alexa Flour 700 goat anti-mouse IgG secondary antibody, mouse anti-Transferrin receptor antibody, DAPI and Prolong Gold were purchased from Invitrogen (Carlsbad, CA). IRDye800CW-labeled anti-rabbit secondary antibody was purchased from LI-COR Biosciences (Lincoln, NE). Mouse anti-α-tubulin antibody and Protein G plus-agarose beads were purchased from Santa Cruz Biotechnology (Santa Cruz, CA). Mouse anti-Myc tag and rabbit anti-IRSp53 antibodies were purchased from Millipore (Bedford, MA). Rabbit anti-GFP tag antibody was purchased from GeneTex (Irvine, CA). ProFection Mammalian Transfection system was purchased from Promega (Madison, WI).

2.2. Plasmids

pEGFP-C1 vector, pRK5-Myc vector, Myc-SH2B1β and GFP-SH2B1β constructs were generous gifts from Professor Christin Carter-Su at the University of Michigan, USA [31,39]. GFP-SH2B1β(1–150), GFP-SH2B1β(270–670), GFP-SH2B1β(397–670) and GFP-SH2B1β(505–670) were made as described in Chen et al. [39]. Full length human IRSp53/pCMV-SPORT6 was purchased from Thermo Fisher Scientific Inc. (Waltham, MA). Full length, N-terminal regions (amino acids 1–374 and 1–251), and C-terminal region (amino acids 286–460) of IRSp53 were sub-cloned into pRK5-Myc via BamHI/EcoRI sites. These constructs were confirmed via enzyme digest as well as DNA sequencing.

2.3. Cell culture, transient transfection and immunofluorescence microscopy

293T cells were purchased from American Type Culture Collection (Manassas, VA). 293T cells were cultured in DMEM containing 10% FBS, 1% L-Gln and 1% AA. The culture condition of the incubator was set in a humidified atmosphere containing 5% CO_2, at 37 °C.

Cells seeded on coverslips and were transfected by ProFection Mammalian Transfection system (Promega) according to the manufacturer's instruction with the indicated expression vectors. Cells were fixed after 24 h using 4% paraformaldehyde, permeabilized, blocked and then incubated with indicated antibodies followed by incubation with Alexa Fluor 488-conjugated IgG and Alexa Fluor 555-conjugated IgG secondary antibodies. Nucleus was detected by staining with DAPI. Cells were mounted with Prolong Gold (Invitrogen). Images were taken using Zeiss LSM 510 confocal microscope system.

Generation of digitalized images was obtained by applying the Adobe Photoshop filter "find edges" to outline the cell contour. Length of the cytoplasmic extension of 293T cells was measured using the Fiji software (http://fiji.sc/), a plugin in ImageJ software. The longest cytoplasmic extension for each cell was compared.

2.4. Immunoblotting and immunoprecipitation

Cells were collected in RIPA buffer (50 mM Tris–HCl, pH 7.5, 150 mM NaCl, 2 mM EGTA, 1% Triton X-100) containing protease inhibitors [1 mM Na_3VO_4, 10 ng/ml leupeptin and 10 ng/ml aprotinin (A + L), 1 mM phenylmethylsulfonyl fluoride (PMSF)]. Equal amount of proteins was loaded and resolved by sodium dodecyl sulfate-polyacrylamide gel electrophoresis (SDS-PAGE) and then transferred to nitrocellulose membrane for Western blotting analysis using the indicated antibodies. For immunoprecipitation, cells were lysed in RIPA buffer containing 1 mM Na_3VO_4, 10 ng/ml A + L, 1 mM PMSF. Cell lysates were incubated with monoclonal anti-Myc tag antibodies (1:200) followed by protein G plus-agarose beads incubation. The immunoprecipitated proteins were subjected to Western blot analysis. The immunoblots were incubated with the indicated antibodies followed by secondary antibodies containing IRDye-conjugated IgG and visualized via Odyssey Infrared Imaging System (LI-COR Biosciences.)

2.5. Subcellular fractionation

Cells were seeded on 10-cm dishes for 1 day and then transfected with the indicated plasmids. One day after transfection, cells were collected in fractionation buffer (10 mM Tris–HCl pH 7.9, 10 mM KCl, 0.1 mM EDTA, 1 mM DTT) containing with 1 mM Na_3VO_4, 1 mM PMSF, 10 ng/ml A + L. Lysates were passed through a 27-G needle 50 times using a 1 ml syringe, and then centrifuged at 2300 rpm (500 ×*g*) at 4 °C for 5 min. After centrifugation, the pellet, designated the nuclear faction (nuclei and nuclei-associated structures), was washed twice by adding 200 μl of fractionation buffer with 0.5% NP-40. Centrifuged again at 3000 rpm at 4 °C for 5 min. Removed the wash buffer, and dispersed by lysis buffer (1% Triton X-100, 1% sodium deoxycholate, 50 mM Tris–HCl, 150 mM NaCl, 1 mM EDTA, 0.1 mM EGTA) containing with 1 mM Na_3VO_4, 1 mM PMSF, 10 ng/ml A + L. The supernatants were centrifuged again at 3000 rpm at 4 °C for 5 min and the supernatant was centrifuged using ultracentrifuge (Hitachi, CS150NX with S80AT3 rotor) at 32,700 rpm (100,000 ×*g*) for 1 h. The resulting supernatants were designated the cytosolic fraction. The pellet, designated membrane fraction, was washed with fractionation buffer and dispersed with lysis buffer.

2.6. Measurement of perimeter length of cells and filopodia number

The perimeter length of cells was measured using the Simple Neurite Tracer, a plugin for ImageJ software. The mean pixel value of perimeter length was measured and converted pixels into micrometers (mm). The number of filopodia was quantified using the built-in cell-counter in ImageJ software. Total numbers of filopodia were divided by perimeter length and times 100 to get #filopodia/100 μm.

2.7. Statistical analysis

The statistical analysis was performed using the paired Student's t-test. Significance (*) is defined as $P < 0.05$.

3. Results

3.1. IMD domain of IRSp53 is critical for filopodium induction in 293 T cells

It is well-established that the expression of full-length IRSp53 or its IMD domain is sufficient to induce filopodium formation in a variety of cell lines such as B16F1, Cos-7, N1E-115 and HeLa cells [10,12,45,46]. Human embryonic kidney 293T cells are good cell model to study the formation of filopodia because they have very low endogenous IRSp53 and exhibit limited filopodia (Fig. 1A and F). We asked whether overexpressing IRSp53 in 293T cells would induce the formation of filopodia of 293T cells. If yes, what region(s) of IRSp53 is required for the formation of filopodia? To this end, various N- and C-terminal truncation mutants fused to Myc tag were constructed. Myc-IRSp53(1–374) contains IMD and CRIB domains. Myc-IRSp53(1–251) contains IMD domain. Myc-IRSp53(286–460) contains SH3 domain (Fig. 1B). The protein expression of these Myc-tagged truncation mutants is shown in Fig. 1C. The effects of IRSp53 and its truncation mutants on the morphology of 293T cells were determined by immunofluorescence staining. As shown in Fig. 1D, overexpression of IRSp53, IRSp53(1–374) and IRSp53(1–251) in 293T cells increased the numbers of filopodium-like

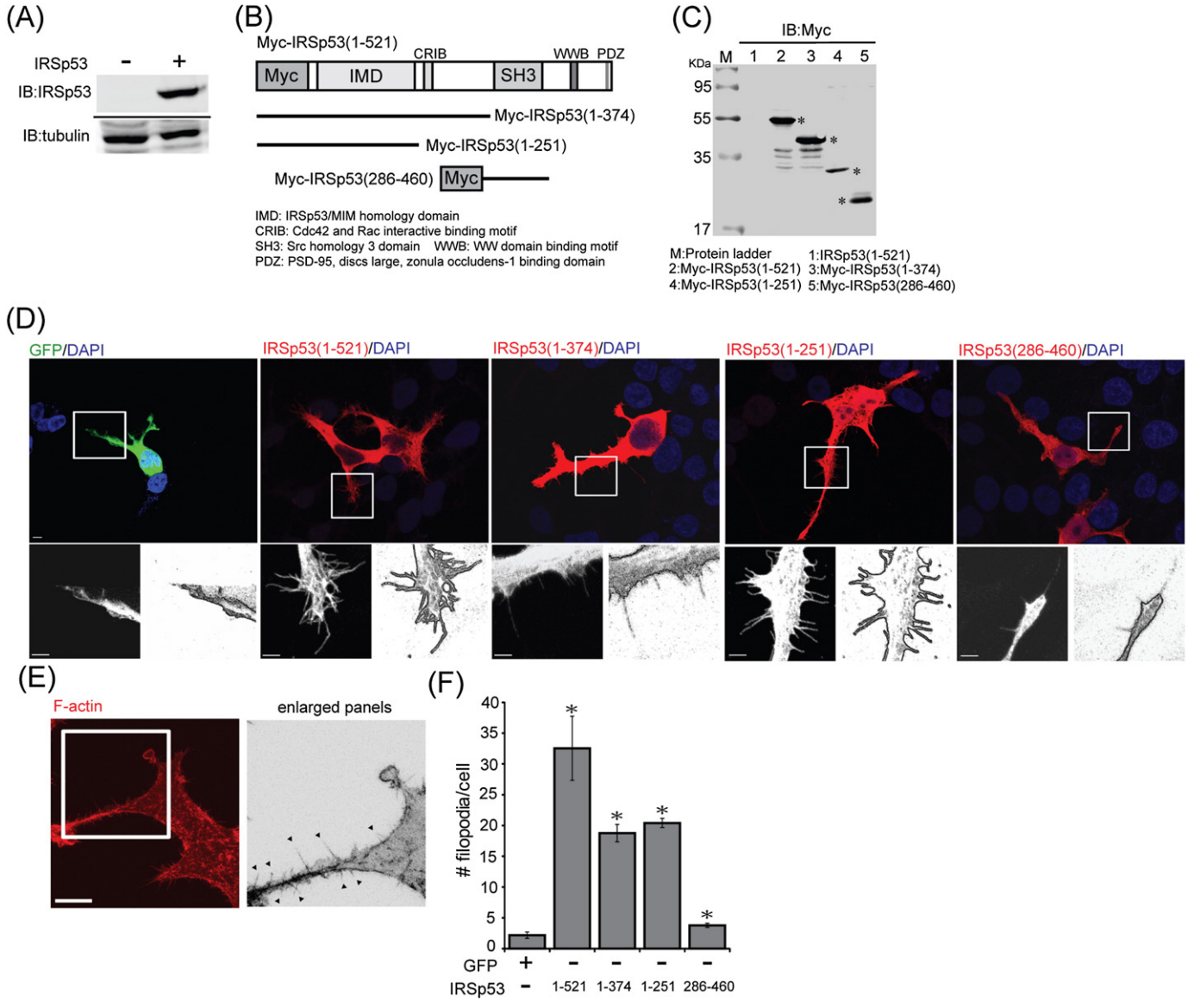

Fig. 1. The IMD domain of IRSp53 induces filopodia of 293T cells. (A) 293T cells were transiently transfected with vector control or Myc-IRSp53. Cell lysates were resolved via SDS-PAGE and immunoblotting using anti-IRSp53 antibody to determine the endogenous versus overexpressed levels of IRSp53. Tubulin was used as a loading control. (B) Schematic representation of full length and truncated human IRSp53 proteins. The Myc tag fused at N-termini and the domain structures are indicated. (C) 293T cells were transiently transfected with IRSp53, Myc-IRSp53, Myc-IRSp53(1–374), Myc-IRSp53(1–251), or Myc-IRSp53(286–460). Cell lysates were analyzed via immunoblotting using anti-Myc antibody. * indicates the overexpressed Myc-fusion proteins. (D) 293T cells transiently transfected with GFP vector, Myc-IRSp53, Myc-IRSp53(1–374), Myc-IRSp53(1–251), or Myc-IRSp53(286–460) were fixed 24 h post-transfection and incubated with anti-Myc antibody to visualize IRSp53 (red), and DAPI to visualize the nucleus (blue). Images were taken using Zeiss LSM 510 confocal microscope. Representative images are shown. The lower panels represent the magnified area indicated in the upper panels (left) and their respective digitalized images (right). Scale bars, 10 μm. (E) 293T cells transiently transfected with GFP-SH2B1β(1–150) were subjected to immunofluorescence staining with rhodamine phalloidin to label F-actin (red). Enlarged images of the filopodia with F-actin staining are shown on the right panels. The arrow heads indicate filopodia. The length of counted filopodia was 2–10 μm. Scale bar = 10 μm. (F) 293T cells were treated as in (D), the average number of filopodia per 100 μm surface length was counted from total 23–25 cells per condition from three independent experiments. The error bars represent S.E.M. The statistical analysis was performed using the paired Student's t-test. *: significant difference compared to GFP only control.

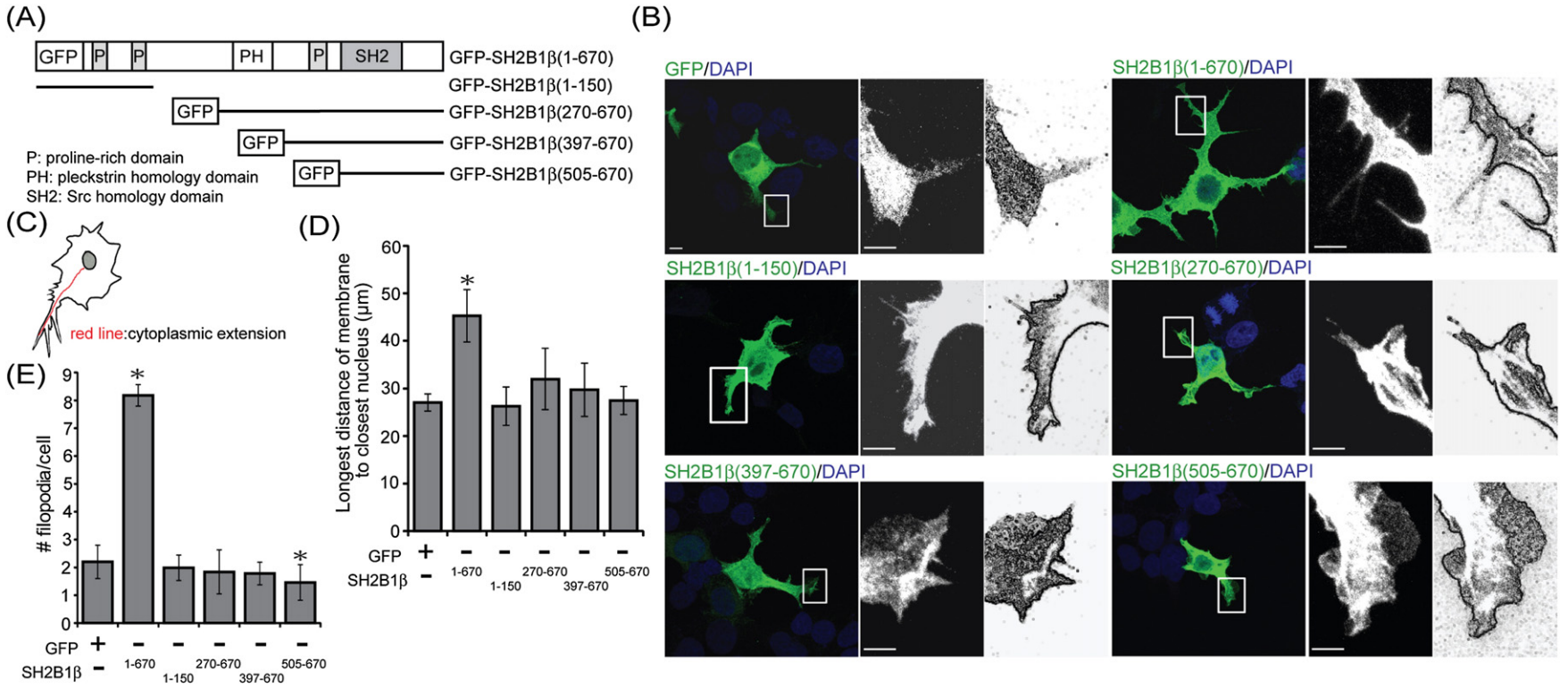

Fig. 2. SH2B1β promotes cytoplasmic extensions of 293T cells. (A) Schematic representation of full length and truncated SH2B1β proteins. The GFP tag was fused to the N-termini of SH2B1β constructs as indicated. (B) 293T cells transiently transfected with GFP, GFP-SH2B1β(1–670), GFP-SH2B1β(1–150), GFP-SH2B1β(270–670), GFP-SH2B1β(397–670), or GFP-SH2B1β(505–670) were fixed 24 h post-transfection and incubated with DAPI to visualize the nucleus (blue). Representative images were taken using Zeiss LSM 510 confocal microscope. The right panels represent magnifications of the areas indicated on the left panels and their respective digitalized images. Scale bars, 10 μm. (C) The extension index was determined by measuring the distance of the longest cytoplasmic extension to the closest nuclear membrane. (D) 293T cells were treated as in (B), cytoplasmic extension of GFP-positive cells were measured using Image J software. The error bars represent S.E.M. from three independent experiments. A total of 50 cells were counted from three independent experiments. (E) 293T cells were treated as in (B), averaged number of filopodia per cell was counted from total 20–23 cells per condition from three independent experiments. The error bars represent S.E.M. The statistical analysis was performed using the paired Student's t-test. *: significant difference compared to GFP only control.

structures, whereas IRSp53(286–460) had mild effect. To determine whether these filopodium-like structures are indeed filopodia, we performed immunofluorescence staining with rhodamine phalloidin to label actin. Actin-positive processes of 2–10 μm long were counted as filopodia in the following experiments (Fig. 1E). Quantified results showed that the number of filopodia in IRSp53-expressing cells was higher than those in IRSp53(1–374)-, IRSp53(1–251)-, or IRSp53(286–460)-expressing cells (Fig. 1F). These results are in line with published reports in other cellular systems and indicate that the IMD domain is required for the induction of filopodia by IRSp53.

3.2. SH2B1β promotes long cytoplasmic extensions to foster more filopodium formation

Our previous results have shown that overexpression of SH2B1β enhances neurite outgrowth of PC12 cells, hippocampal and cortical neurons [34,35]. During neurogenesis, filopodium formation is required for neurite initiation [44]. It is thus of interest to know if SH2B1β regulates the formation of filopodia. To this end, wild type as well as previously constructed GFP-tagged N- and C-terminal truncation mutants of SH2B1β were transfected to 293T cells and the numbers of filopodia were counted. SH2B1β(1–150) contains dimerization domain (DD) and two proline-rich domains. SH2B1β(270–670) contains PH, proline-rich and SH2 domains. SH2B1β(397–670) contains C-terminal proline-rich and SH2 domain. SH2B1β(505–670) contains SH2 domain (Fig. 2A). Cells transiently transfected with various GFP-fused SH2B1β constructs were fixed 24 h post-transfection and cell morphology was imaged and analyzed. As shown in Fig. 2B, overexpression of SH2B1β increased cytoplasmic extension as well as the number of filopodia compared to GFP-expressing control cells. The extension index was determined by measuring the distance of the longest cytoplasmic extension to the closest nuclear membrane (Fig. 2C). Quantification results showed that SH2B1β, but not other SH2B1β mutants, significantly increased cytoplasmic extension (Fig. 2D). Quantification of the filopodium numbers revealed that SH2B1β significantly enhanced the number of filopodia, whereas other mutants did not (Fig. 2E). The fact that many filopodia generated from the long cytoplasmic extension suggest the possibility that SH2B1β promotes long cytoplasmic extensions to foster the formation of filopodia.

3.3. A positive role of SH2B1β in IRSp53-mediated filopodium formation

The fact that both IRSp53 and SH2B1β can increase the number of filopodia, we next examined whether IRSp53 and SH2B1β could synergistically increase the number of filopodia. To this end, IRSp53, SH2B1β alone, or in combination were transfected to 293T cells. Morphology of 293T cells overexpressing Myc-IRSp53 or GFP-SH2B1β alone, or in combination, was determined by immunofluorescence staining. Consistent with the results from Figs. 1–2, overexpression of either IRSp53 or SH2B1β increases the number of filopodia. The number of filopodia in IRSp53-expressing cells was higher than those in SH2B1β-expressing cells, suggesting that IRSp53 is a stronger inducer of filopodium formation. Interestingly, co-expression of both IRSp53 and SH2B1β further increased the numbers of the filopodia, suggesting that IRSp53 and SH2B1β synergistically enhanced filopodium formation (Fig. 3A). Similar to Fig. 2, SH2B1β appears to increase the area of membrane by facilitating cytoplasmic extension. Representative images as well as digitalized images are shown to highlight the contour of cells (Fig. 3B). These results suggest that IRSp53 and SH2B1β synergistically increase the number of filopodia.

3.4. IRSp53 interacts with SH2B1β

The fact that SH2B1β and IRSp53 synergistically increase the number of filopodia suggests that SH2B1β may interact with IRSp53 or these two proteins are in the same complexes. To this end, GFP-SH2B1β alone, or together with various Myc-tagged IRSp53 constructs (as shown in Fig. 1B) were transiently transfected to 293T cells and immunoprecipitated with anti-Myc antibody to pull down IRSp53-containing complexes. As shown in Fig. 4A, SH2B1β interacted with full-length IRSp53 and IRSp53(286–460). Both full-length IRSp53 and IRSp53(286–460) contain SH3 domain, suggesting that IRSp53 may interact with SH2B1β through its SH3 domain. We next determine whether the N-terminal of SH2B1β, containing two proline-rich domains, could potentially be the interaction

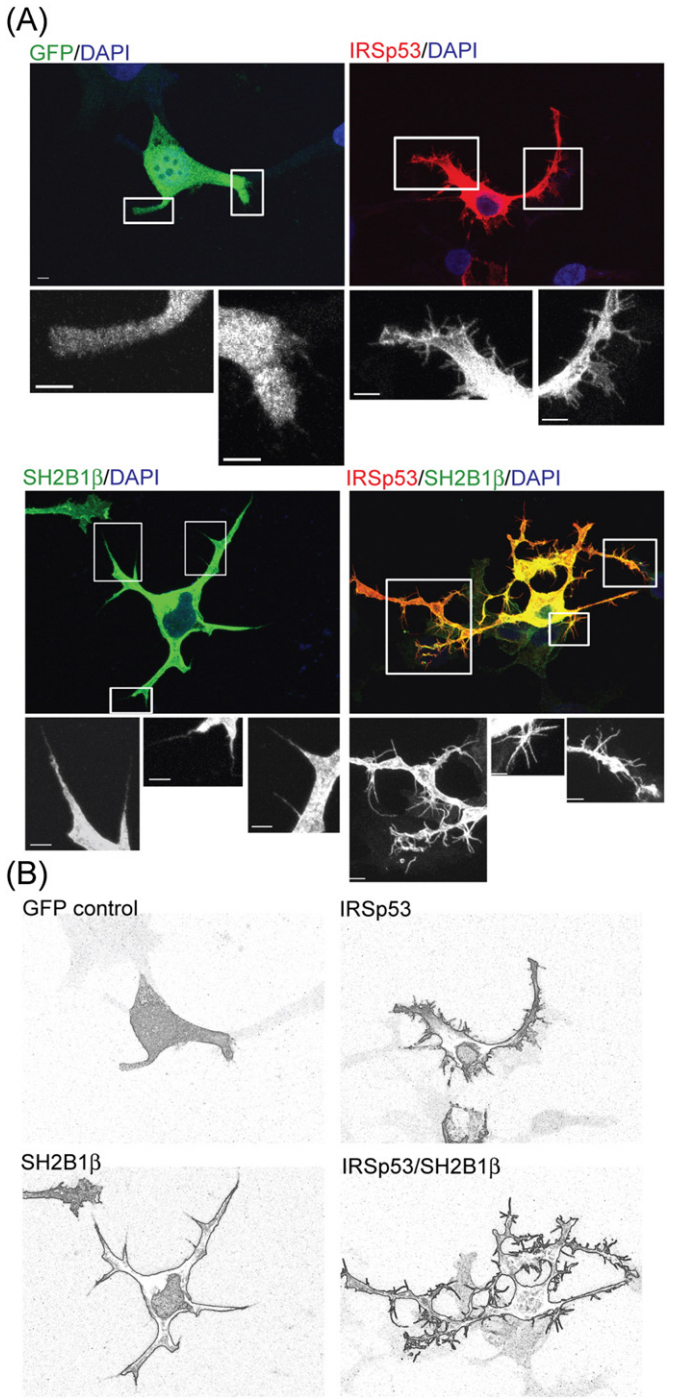

Fig. 3. Role of IRSp53 and SH2B1β in the formation of filopodia. (A) 293T cells transiently transfected with GFP, GFP-SH2B1β or Myc-IRSp53 alone or in combination were fixed at 24 h post-transfection and incubated with anti-IRSp53 antibody to visualize IRSp53 (red), DAPI to visualize the nucleus (blue). Green fluorescence represents GFP-SH2B1β. Representative images were taken using Zeiss LSM 510 confocal microscope. The bottom panels represent magnifications of the areas indicated in the top panels. Scale bars, 10 μm. (B) Digitalized analysis used Adobe Photoshop filters to highlight the contour of cells from (A) to show membrane protrusions.

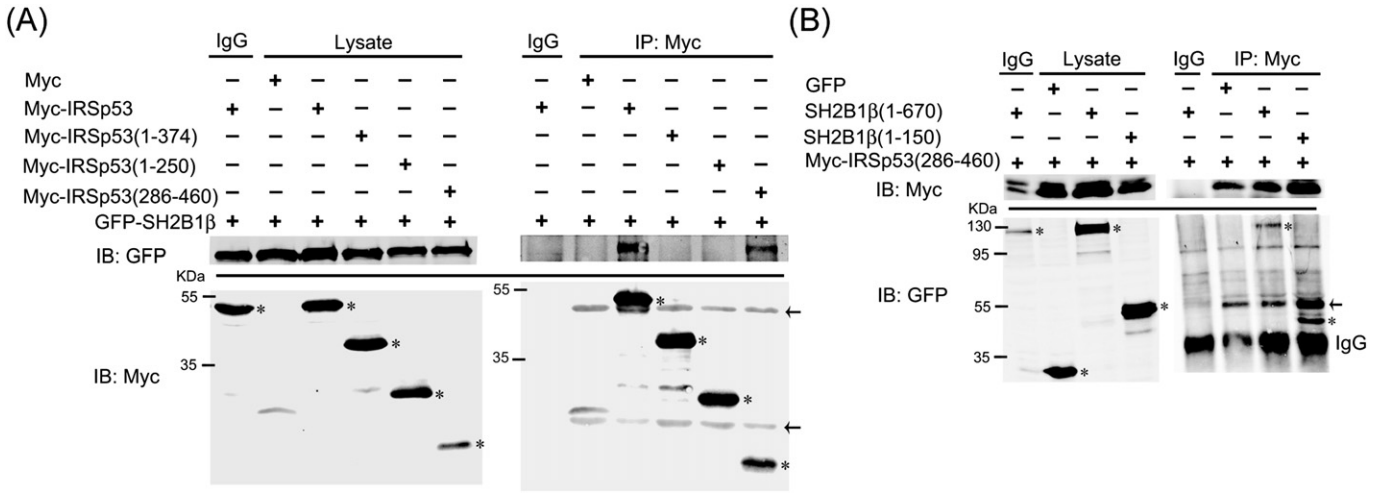

Fig. 4. IRSp53 interacts with SH2B1β. (A) 293T cells were transfected with Myc vector, GFP-SH2B1β alone, or together with various Myc-tagged IRSp53 constructs (shown in Fig. 1B). Cell lysates were collected and subjected to immunoprecipitation using anti-Myc antibody followed by immunoblotting with anti-GFP or anti-Myc antibody. Left panels are cell lysate controls. (B) 293T cells were transfected with GFP, Myc-IRSp53(286–460) alone, or together with GFP-SH2B1β or GFP-SH2B1β(1–150). Cell lysates were collected subjected to immunoprecipitation using anti-Myc antibody followed by immunoblotting with anti-GFP or anti-Myc antibody. Left panels are cell lysate controls. Specific bands are indicated by the asterisks and non-specific bands are indicated by the arrows.

region with IRSp53. To this end, Myc-IRSp53(286–460) together with GFP vector, GFP-SH2B1β or GFP-SH2B1β(1–150) were transiently transfected to 293T cells and immunoprecipitated with anti-Myc antibody. As shown in Fig. 4B, the SH3 domain of IRSp53 interacted with both full length SH2B1β and the N-terminal proline-rich domains of SH2B1β. Thus, it is likely that the SH3 domain of IRSp53 is responsible for interacting with N-terminal proline-rich domains of SH2B1β.

3.5. N-terminal proline-rich domains of SH2B1β are not sufficient to enhance IRSp53-induced filopodia

The fact that SH2B1β and IRSp53 can form a complex to enhance filopodium formation, we next examine which domain(s) of SH2B1β is required for this enhancement. To this end, 293T cells were transiently transfected with IRSp53 alone, or together with various GFP-tagged truncation mutants of SH2B1β (as shown in Fig. 2A), cell morphology was assessed. As shown in Fig. 5A, overexpression of IRSp53 alone induced filopodium formation. Co-expression of full length SH2B1β significantly enhanced IRSp53-induced filopodium formation 2-fold (Fig. 5A-B). Interestingly, co-expressing SH2B1β(1–150) and IRSp53 also increased the number of filopodia compared to IRSp53-overexpressing cells (Fig. 5A–B). To discern whether SH2B1β directly increases the number of filopodia or indirectly through increasing perimeter of cells, cell perimeter was measured and the numbers of filopodia per 100 μm surface length was calculated. As shown in Fig. 5C, only full length SH2B1β significantly increased the number of filopodia/100 μm. These results suggest that the interaction with IRSp53 is not sufficient to increase the number of filopodia. Other domains of SH2B1β are required for the positive regulation.

3.6. Both N- and C-termini of IRSp53 are required to increase SH2B1β-induced filopodia

To determine which domain(s) of IRSp53 is required for enhancing SH2B1β-induced formation of filopodia, 293T cells were transiently transfected with SH2B1β alone, or together with various Myc-tagged IRSp53 constructs (as shown in Fig. 1B). Consistent with results from Figs. 2–3, overexpression of SH2B1β promoted cytoplasmic extension whereas co-expressing SH2B1β and IRSp53 synergistically increased the numbers of filopodia (Fig. 6A). The increased numbers of filopodia were observed in cells expressing SH2B1β together with IRSp53(1–521), IRSp53(1–374), or IRSp53(1–251) (Fig. 6A–B). Interestingly, co-expression of SH2B1β and IRSp53(286–460), which contains SH3 domain that interacts with SH2B1β, did not enhance SH2B1-induced filopodium numbers (Fig. 6A–B). The numbers of filopodia per 100 μm cell surface were also calculated. As shown in Fig. 6C, SH2B1β alone did not increase the number of filopodia per 100 μm surface length. IRSp53(1–521), IRSp53(1–374), IRSp53(1–251) and IRSp53(286–460), on the other hand, all can significantly increase the number of filopodia per 100 μm surface length in the presence of SH2B1β. These results suggest that IMD and CRIB domains of IRSp53 exhibited more positive effect on SH2B1β-mediated filopodium formation. Increasing filopodia requires cytoplasmic extension to generate more membrane surface for new filopodium formation. Overexpressing IRSp53 enhanced SH2B1β-induced filopodia much more than IMD domain-only construct suggesting a role for SH3 domain in promoting SH2B1β-induced filopodium formation. By considering the perimeter of cells, SH3 domain of IRSp53 in deed increased the number of filopodia in the presence of SH2B1β, though to a lesser extent. Nonetheless, these results suggest that IMD domain-mediated membrane deformation is required for SH3 domain-mediated effect.

3.7. IRSp53 may modulate the subcellular distribution of SH2B1β

To deform plasma membrane for the initiation of filopodia, the responsible protein complexes in theory should localize to plasma membrane. To determine the subcellular distribution of IRSp53 and SH2B1β, lysates of 293T cells transiently transfected with GFP-SH2B1β, Myc-IRSp53 or in combination were subjected to subcellular fractionation. Overexpression of SH2B1β did not affect the plasma membrane distribution of IRSp53 when compared with expression of IRSp53 alone (Fig. 7, left panels). Interestingly, overexpressing IRSp53 increased membrane distribution of SH2B1β by 10-fold (Fig. 7, right panels). These results suggest that IRSp53 may recruit SH2B1β to the plasma membrane to participate membrane elongation and protrusion.

4. Discussion

Filopodia are considered to be precursors of polarized structures such as synapses and neurites [44,47]. In this study, we characterized SH2B1β as a binding partner of IRSp53 and synergistically increased the numbers of filopodia for 293T cells. Although SH2B1β binds to

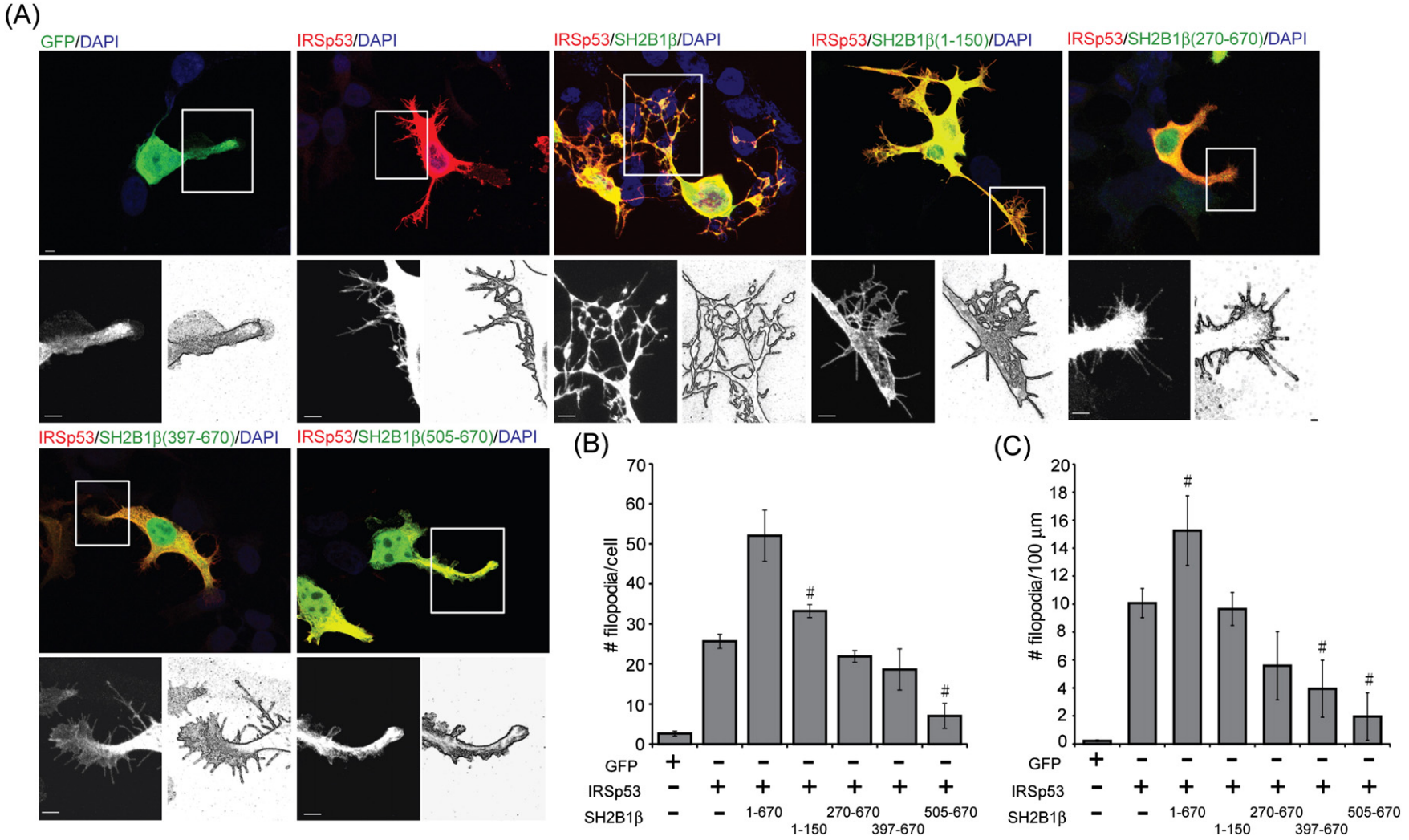

Fig. 5. Effect of expressing various truncation constructs of GFP-tagged SH2B1β and Myc-IRSp53 on filopodium formation. (A) 293T cells transiently transfected with GFP, Myc-IRSp53 alone, or together with various GFP-tagged constructs of SH2B1β (shown in Fig. 2A) were fixed 24 h post-transfection and incubated with anti-Myc antibody to visualize IRSp53 (red), DAPI to visualize the nucleus (blue). Images were taken using Zeiss LSM 510 confocal microscope. Representative images are shown. The lower panels represent magnifications of the areas indicated in the upper panels (left) and their respective digitalized images (right). Scale bars, 10 μm. (B) 293T cells were treated as in (A), the average number of filopodia was counted from total 21–25 cells per condition from three independent experiments. The error bars represent S.E.M. The statistical analysis was performed using the paired Student's t-test. #: significant difference compared to IRSp53 only control. (C) 293T cells were treated as in (A), the number of filopodia was quantified per 100 μm cell surface. A total of 21–25 cells were counted per condition from three independent experiments. Values are mean ± S.E.M. The statistical analysis was performed using the paired Student's t-test. #: significant difference compared to IRSp53 only control.

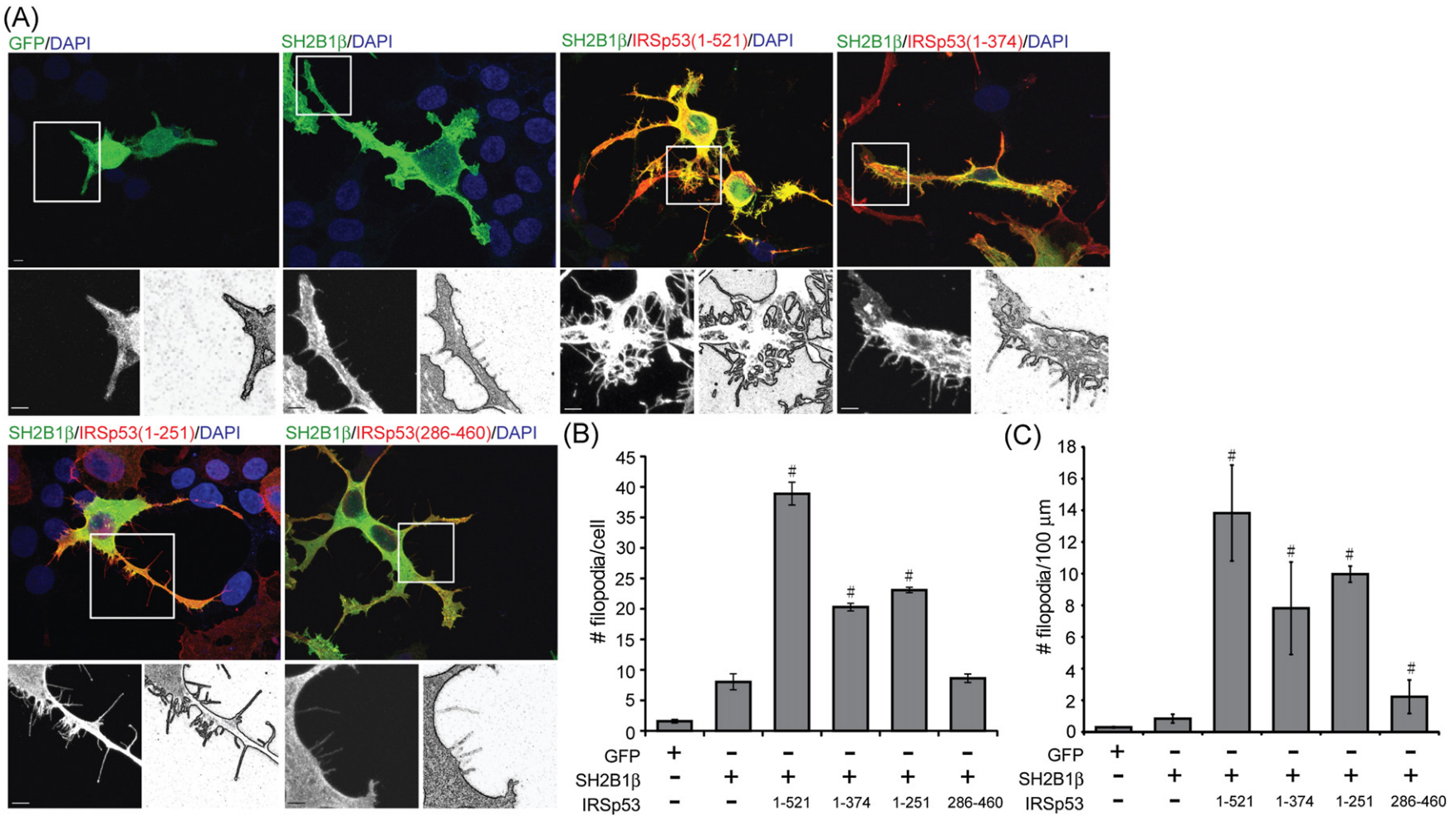

Fig. 6. Overexpression of GFP-SH2B1β in the presence of various truncation constructs of Myc-tagged IRSp53 increases the number of filopodia. (A) 293T cells transiently transfected with GFP, GFP-SH2B1β alone, or together with various Myc-tagged constructs of IRSp53 (shown in Fig. 1B) were fixed 24 h post-transfection and incubated with anti-Myc antibody to visualize IRSp53 truncations (red), DAPI to visualize the nucleus (blue). Images were taken using Zeiss LSM 510 confocal microscope. Representative images are shown. The lower panels represent magnifications of the areas indicated in the upper panels (left) and their respective digitalized images (right). Scale bars, 10 μm. (B) 293T cells were treated as in (A), the average number of filopodia was counted from total 19–24 cells per condition from three independent experiments. The error bars represent S.E.M. The statistical analysis was performed using the paired Student's t-test. #: significant difference compared to SH2B1β only control. (C) 293T cells were treated as in (A), the numbers of filopodia were quantified per 100 μm cell surface. A total of 19–24 cells were counted per condition from three independent experiments. Values are mean ± S.E.M. The statistical analysis was performed using the paired Student's t-test. #: significant difference compared to SH2B1β only control.

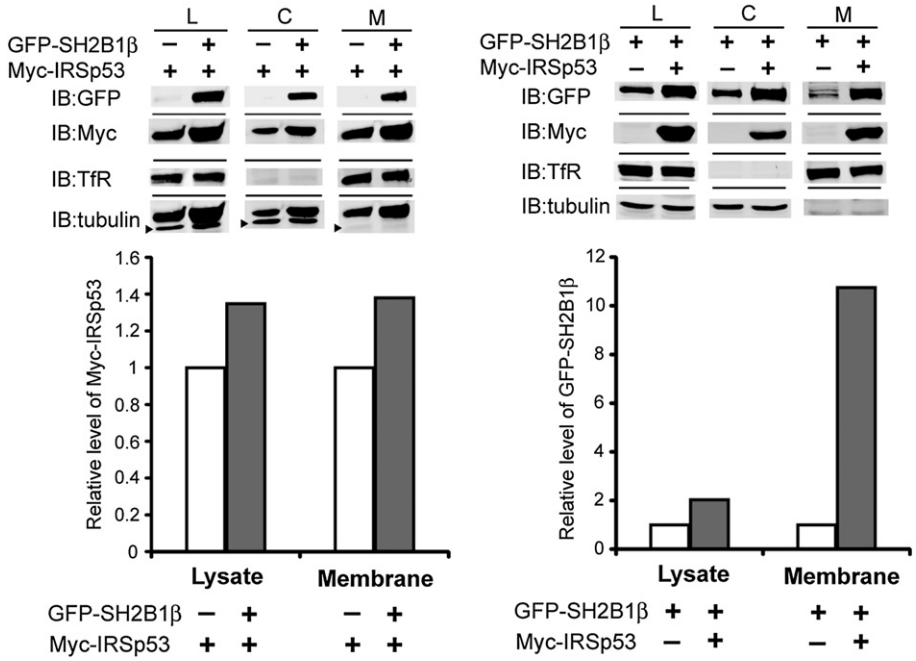

Fig. 7. Sub-cellular distribution of IRSp53 and SH2B1β in 293T cells. Cell lysates from 293T cells transfected with GFP-SH2B1β, Myc-IRSp53 or in combination were extracted followed by subcellular fractionation. The whole cell lysate (designated as L) and two fractions were shown, membrane fraction (designated as M), cytoplasmic fraction (designated as C). Samples were resolved via SDS-PAGE and immunoblotting with anti-GFP, Myc, transferrin receptor (designated as TfR), or α-tubulin antibody. α-Tubulin and TfR are shown as loading controls for whole cell lysates and membrane fraction, respectively.

IRSp53 through its N-terminal proline-rich regions, this interaction domain is not sufficient to increase the number of filopodia (Fig. 5C). It is possible that the reported actin-binding region between a.a. 150 and 200 of SH2B1β is required for the enhancement [43]. However, comparing to SH2B1β(1–150), SH2B1β(1–260) did not show further enhancement of neurite numbers and branching for hippocampal neurons (unpublished results). Both IRSp53 and SH2B1β bind to actin. Thus, it is yet to be determined whether the actin-binding ability of SH2B1β or IRSp53 is required for the increased numbers of filopodia.

Overexpression of full length or mutants of IRSp53 increases the number of filopodia in the presence of SH2B1β. This positive regulation requires cytoplasmic extension driven mainly by SH2B1β (Fig. 2). Considering the number of filopodia per cell perimeter, SH2B1β alone did not increase the number of filopodia per 100 μm surface length (Fig. S1). Filopodium formation is likely driven by IRSp53 because IRSp53 and its mutants can increase the number of filopodia per 100 μm surface length (Fig. S2). Expressing IRSp53(1–374) or IRSp53(1–251) generated similar numbers of filopodia (Fig. 6B–C), suggesting that CRIB domain of IRSp53 may not play a significant role in SH2B1β-mediated filopodium formation. IMD domain is the main region that promotes membrane protrusion. SH3 domain of IRSp53 interacts with SH2B1β. Our fractionation results suggest that IRSp53 recruits SH2B1β to the plasma membrane, possibly to promote membrane elongation and protrusion. This finding also reveals a novel mechanism of SH2B1 targeting suggesting that it can be recruited to plasma membrane by proteins other than receptor tyrosine kinases and signaling molecules.

Acknowledgements

We thank Dr. Eric Huang from the National Chiao Tung University and Dr. Jui-Chou Hsu from the National Tsing Hua University in Taiwan, for the insightful discussion concerning this project. This study was supported by grants from the National Science Council of Taiwan (NSC101-2311-B-007-012-MY3), and National Health Research Institutes (NHRI-EX103-10206NI).

Appendix A. Supplementary data

Supplementary data to this article can be found online at http://dx.doi.org/10.1016/j.bbagen.2014.08.011.

References

[1] R.C. May, The Arp2/3 complex: a central regulator of the actin cytoskeleton, Cell. Mol. Life Sci. 58 (2001) 1607–1626.
[2] R.C. May, L.M. Machesky, Phagocytosis and the actin cytoskeleton, J. Cell Sci. 114 (2001) 1061–1077.
[3] T.H. Millard, S.J. Sharp, L.M. Machesky, Signalling to actin assembly via the WASP (Wiskott–Aldrich syndrome protein)-family proteins and the Arp2/3 complex, Biochem. J. 380 (2004) 1–17.
[4] T.M. Svitkina, E.A. Bulanova, O.Y. Chaga, D.M. Vignjevic, S. Kojima, J.M. Vasiliev, G.G. Borisy, Mechanism of filopodia initiation by reorganization of a dendritic network, J. Cell Biol. 160 (2003) 409–421.
[5] A. Hall, Rho GTPases and the actin cytoskeleton, Science 279 (1998) 509–514.
[6] R. Rohatgi, L. Ma, H. Miki, M. Lopez, T. Kirchhausen, T. Takenawa, M.W. Kirschner, The interaction between N-WASP and the Arp2/3 complex links Cdc42-dependent signals to actin assembly, Cell 97 (1999) 221–231.
[7] T.C. Yeh, W. Ogawa, A.G. Danielsen, R.A. Roth, Characterization and cloning of a 58/53-kDa substrate of the insulin receptor tyrosine kinase, J. Biol. Chem. 271 (1996) 2921–2928.
[8] S. Govind, R. Kozma, C. Monfries, L. Lim, S. Ahmed, Cdc42Hs facilitates cytoskeletal reorganization and neurite outgrowth by localizing the 58-kD insulin receptor substrate to filamentous actin, J. Cell Biol. 152 (2001) 579–594.
[9] S. Krugmann, I. Jordens, K. Gevaert, M. Driessens, J. Vandekerckhove, A. Hall, Cdc42 induces filopodia by promoting the formation of an IRSp53:Mena complex, Curr. Biol. 11 (2001) 1645–1655.
[10] H. Nakagawa, H. Miki, M. Nozumi, T. Takenawa, S. Miyamoto, J. Wehland, J.V. Small, IRSp53 is colocalised with WAVE2 at the tips of protruding lamellipodia and filopodia independently of Mena, J. Cell Sci. 116 (2003) 2577–2583.
[11] T.H. Millard, G. Bompard, M.Y. Heung, T.R. Dafforn, D.J. Scott, L.M. Machesky, K. Futterer, Structural basis of filopodia formation induced by the IRSp53/MIM homology domain of human IRSp53, EMBO J. 24 (2005) 240–250.
[12] A. Disanza, S. Mantoani, M. Hertzog, S. Gerboth, E. Frittoli, A. Steffen, K. Berhoerster, H.J. Kreienkamp, F. Milanesi, P.P. Di Fiore, A. Ciliberto, T.E. Stradal, G. Scita, Regulation of cell shape by Cdc42 is mediated by the synergic actin-bundling activity of the Eps8–IRSp53 complex, Nat. Cell Biol. 8 (2006) 1337–1347.
[13] L.M. Machesky, S.A. Johnston, MIM: a multifunctional scaffold protein, J Mol Med (Berl) 85 (2007) 569–576.
[14] P.K. Mattila, A. Pykalainen, J. Saarikangas, V.O. Paavilainen, H. Vihinen, E. Jokitalo, P. Lappalainen, Missing-in-metastasis and IRSp53 deform PI(4,5)P2-rich membranes by an inverse BAR domain-like mechanism, J. Cell Biol. 176 (2007) 953–964.

[15] S. Suetsugu, K. Murayama, A. Sakamoto, K. Hanawa-Suetsugu, A. Seto, T. Oikawa, C. Mishima, M. Shirouzu, T. Takenawa, S. Yokoyama, The RAC binding domain/IRSp53-MIM homology domain of IRSp53 induces RAC-dependent membrane deformation, J. Biol. Chem. 281 (2006) 35347–35358.
[16] J. Saarikangas, H. Zhao, A. Pykalainen, P. Laurinmaki, P.K. Mattila, P.K. Kinnunen, S.J. Butcher, P. Lappalainen, Molecular mechanisms of membrane deformation by I-BAR domain proteins, Curr. Biol. 19 (2009) 95–107.
[17] S. Suetsugu, S. Kurisu, T. Oikawa, D. Yamazaki, A. Oda, T. Takenawa, Optimization of WAVE2 complex-induced actin polymerization by membrane-bound IRSp53, PIP(3), and Rac, J. Cell Biol. 173 (2006) 571–585.
[18] H. Miki, H. Yamaguchi, S. Suetsugu, T. Takenawa, IRSp53 is an essential intermediate between Rac and WAVE in the regulation of membrane ruffling, Nature 408 (2000) 732–735.
[19] H. Miki, T. Takenawa, WAVE2 serves a functional partner of IRSp53 by regulating its interaction with Rac, Biochem. Biophys. Res. Commun. 293 (2002) 93–99.
[20] Y. Funato, T. Terabayashi, N. Suenaga, M. Seiki, T. Takenawa, H. Miki, IRSp53/Eps8 complex is important for positive regulation of Rac and cancer cell motility/invasiveness, Cancer Res. 64 (2004) 5237–5244.
[21] T. Fujiwara, A. Mammoto, Y. Kim, Y. Takai, Rho small G-protein-dependent binding of mDia to an Src homology 3 domain-containing IRSp53/BAIAP2, Biochem. Biophys. Res. Commun. 271 (2000) 626–629.
[22] Y. Okamura-Oho, T. Miyashita, K. Ohmi, M. Yamada, Dentatorubral-pallidoluysian atrophy protein interacts through a proline-rich region near polyglutamine with the SH3 domain of an insulin receptor tyrosine kinase substrate, Hum. Mol. Genet. 8 (1999) 947–957.
[23] J. Bockmann, M.R. Kreutz, E.D. Gundelfinger, T.M. Bockers, ProSAP/Shank postsynaptic density proteins interact with insulin receptor tyrosine kinase substrate IRSp53, J. Neurochem. 83 (2002) 1013–1017.
[24] M. Soltau, D. Richter, H.J. Kreienkamp, The insulin receptor substrate IRSp53 links postsynaptic shank1 to the small G-protein cdc42, Mol. Cell. Neurosci. 21 (2002) 575–583.
[25] D.J. Kast, C. Yang, A. Disanza, M. Boczkowska, Y. Madasu, G. Scita, T. Svitkina, R. Dominguez, Mechanism of IRSp53 inhibition and combinatorial activation by Cdc42 and downstream effectors, Nat. Struct. Mol. Biol. 21 (2014) 413–422.
[26] N. Yousaf, Y. Deng, Y. Kang, H. Riedel, Four PSM/SH2-B alternative splice variants and their differential roles in mitogenesis, J. Biol. Chem. 276 (2001) 40940–40948.
[27] H. Riedel, J. Wang, H. Hansen, N. Yousaf, PSM, an insulin-dependent, pro-rich, PH, SH2 domain containing partner of the insulin receptor, J. Biochem. 122 (1997) 1105–1113.
[28] L. Rui, L.S. Mathews, K. Hotta, T.A. Gustafson, C. Carter-Su, Identification of SH2-Bbeta as a substrate of the tyrosine kinase JAK2 involved in growth hormone signaling, Mol. Cell. Biol. 17 (1997) 6633–6644.
[29] L. Rui, C. Carter-Su, Platelet-derived growth factor (PDGF) stimulates the association of SH2-Bbeta with PDGF receptor and phosphorylation of SH2-Bbeta, J. Biol. Chem. 273 (1998) 21239–21245.
[30] J. Wang, H. Riedel, Insulin-like growth factor-I receptor and insulin receptor association with a Src homology-2 domain-containing putative adapter, J. Biol. Chem. 273 (1998) 3136–3139.
[31] L. Rui, J. Herrington, C. Carter-Su, SH2-B is required for nerve growth factor-induced neuronal differentiation, J. Biol. Chem. 274 (1999) 10590–10594.
[32] Y. Zhang, W. Zhu, Y.G. Wang, X.J. Liu, L. Jiao, X. Liu, Z.H. Zhang, C.L. Lu, C. He, Interaction of SH2-Bbeta with RET is involved in signaling of GDNF-induced neurite outgrowth, J. Cell Sci. 119 (2006) 1666–1676.
[33] S. Donatello, A. Fiorino, D. Degl'Innocenti, L. Alberti, C. Miranda, L. Gorla, I. Bongarzone, M.G. Rizzetti, M.A. Pierotti, M.G. Borrello, SH2B1beta adaptor is a key enhancer of RET tyrosine kinase signaling, Oncogene 26 (2007) 6546–6559.
[34] W.F. Lin, C.J. Chen, Y.J. Chang, S.L. Chen, I.M. Chiu, L. Chen, SH2B1beta enhances fibroblast growth factor 1 (FGF1)-induced neurite outgrowth through MEK–ERK1/2-STAT3–Egr1 pathway, Cell. Signal. 21 (2009) 1060–1072.
[35] C.H. Shih, C.J. Chen, L. Chen, New function of the adaptor protein SH2B1 in brain-derived neurotrophic factor-induced neurite outgrowth, PLoS One 8 (2013) e79619.
[36] K. Nelms, T.J. O'Neill, S. Li, S.R. Hubbard, T.A. Gustafson, W.E. Paul, Alternative splicing, gene localization, and binding of SH2-B to the insulin receptor kinase domain, Mamm. Genome 10 (1999) 1160–1167.
[37] T.C. Wang, Y.H. Li, K.W. Chen, C.J. Chen, C.L. Wu, N.Y. Teng, L. Chen, SH2B1beta regulates N-cadherin levels, cell–cell adhesion and nerve growth factor-induced neurite initiation, J. Cell. Physiol. 226 (2011) 2063–2074.
[38] W.C. Lu, C.J. Chen, H.C. Hsu, H.L. Hsu, L. Chen, The adaptor protein SH2B1beta reduces hydrogen peroxide-induced cell death in PC12 cells and hippocampal neurons, J. Mol. Signal. 5 (2010) 17.
[39] L. Chen, C. Carter-Su, Adapter protein SH2-B beta undergoes nucleocytoplasmic shuttling: implications for nerve growth factor induction of neuronal differentiation, Mol. Cell. Biol. 24 (2004) 3633–3647.
[40] L. Chen, T.J. Maures, H. Jin, J.S. Huo, S.A. Rabbani, J. Schwartz, C. Carter-Su, SH2B1beta (SH2-Bbeta) enhances expression of a subset of nerve growth factor-regulated genes important for neuronal differentiation including genes encoding urokinase plasminogen activator receptor and matrix metalloproteinase 3/10, Mol. Endocrinol. 22 (2008) 454–476.
[41] Y.J. Chang, K.W. Chen, C.J. Chen, M.H. Lin, Y.J. Sun, J.L. Lee, I.M. Chiu, L. Chen, SH2B1beta interacts with STAT3 and enhances fibroblast growth factor 1-induced gene expression during neuronal differentiation, Mol. Cell. Biol. 34 (2014) 1003–1019.
[42] J. Herrington, M. Diakonova, L. Rui, D.R. Gunter, C. Carter-Su, SH2-B is required for growth hormone-induced actin reorganization, J. Biol. Chem. 275 (2000) 13126–13133.
[43] L. Rider, J. Tao, S. Snyder, B. Brinley, J. Lu, M. Diakonova, Adapter protein SH2B1beta cross-links actin filaments and regulates actin cytoskeleton, Mol. Endocrinol. 23 (2009) 1065–1076.
[44] E.W. Dent, A.V. Kwiatkowski, L.M. Mebane, U. Philippar, M. Barzik, D.A. Rubinson, S. Gupton, J.E. Van Veen, C. Furman, J. Zhang, A.S. Alberts, S. Mori, F.B. Gertler, Filopodia are required for cortical neurite initiation, Nat. Cell Biol. 9 (2007) 1347–1359.
[45] A. Yamagishi, M. Masuda, T. Ohki, H. Onishi, N. Mochizuki, A novel actin bundling/filopodium-forming domain conserved in insulin receptor tyrosine kinase substrate p53 and missing in metastasis protein, J. Biol. Chem. 279 (2004) 14929–14936.
[46] W.I. Goh, K.B. Lim, T. Sudhaharan, K.P. Sem, W. Bu, A.M. Chou, S. Ahmed, mDia1 and WAVE2 proteins interact directly with IRSp53 in filopodia and are involved in filopodium formation, J. Biol. Chem. 287 (2012) 4702–4714.
[47] N.E. Ziv, S.J. Smith, Evidence for a role of dendritic filopodia in synaptogenesis and spine formation, Neuron 17 (1996) 91–102.